# *Nonendocytic Delivery of Functional Engineered Nanoparticles into the Cytoplasm of Live Cells Using a Novel, High-Throughput Microfluidic Device*

Published in final edited form as:
*Nano Lett*. 2012 December 12; 12(12): 6322–6327. doi:10.1021/nl303421h.

# Non-endocytic delivery of functional engineered nanoparticles into the cytoplasm of live cells using a novel, high-throughput microfluidic device

**Jungmin Lee**[1,‡], **Armon Sharei**[2,‡], **Woo Young Sim**[2], **Andrea Adamo**[2], **Robert Langer**[2], **Klavs F. Jensen**[2], and **Moungi G. Bawendi**[1,*]

[1]Department of Chemistry, 77 Massachusetts Avenue, Massachusetts Institute of Technology (MIT), Cambridge, MA 02139 USA

[2]Department of Chemical Engineering, 77 Massachusetts Avenue, Massachusetts Institute of Technology (MIT), Cambridge, MA 02139 USA

## Abstract

The ability to straightforwardly deliver engineered nanoparticles into the cell cytosol with high viability will vastly expand the range of biological applications. Nanoparticles could potentially be used as delivery vehicles or as fluorescent sensors to probe the cell. In particular, quantum dots (QDs) may be used to illuminate cytosolic proteins for long-term microscopy studies. Whereas recent advances have been successful in specifically labeling proteins with QDs on the cell membrane, cytosolic delivery of QDs into live cells has remained challenging. In this report, we demonstrate high throughput delivery of QDs into live cell cytoplasm using an uncomplicated microfluidic device while maintaining cell viabilities of 80–90%. We verify that the nanoparticle surface interacts with the cytosolic environment and that the QDs remain non-aggregated so that single QDs can be observed.

### Keywords

QD; cytosolic delivery; microfluidic device; single QD tracking

Engineered nanomaterials have immense potential as live cell imaging tools, therapeutic molecular delivery agents, or even as ways to manipulate live cells with external handles such as light or magnetic fields.[1] But much of these potential applications require that nanomaterials be delivered into the cell cytosol. For example, quantum dots (QDs) as fluorescent labels have provided new insights into cellular processes such as the dynamics of receptor proteins.[2,3] However, these applications have thus far been limited to proteins localized on the outer cell membrane. Most nanoparticles, such as QDs, need to be passivated with a polymer that renders the nanoparticles soluble in aqueous media, and this also generally prevents them from passively diffusing across the cell membrane. Microinjection and nanoneedle injection[4,5] of nanoparticles is considered impractical due to

*Corresponding Author: mgb@mit.edu Phone: +1-617-253-9796 Fax: +1-617-253-7030.
‡**Author Contributions**
These authors contributed equally to this work.

**Notes**
The authors declare no competing financial interests.

Supporting information
Detailed information on QD construct design and synthesis, cellular delivery and imaging, image and data processing, additional construct and control data are available free of charge via the internet at http://pubs.acs.org.

specialized equipment/skills required and low throughput,[6,7] while electroporation[8,9] may cause QD aggregation inside the cell. Therefore, most attempts to deliver QDs into the cell cytoplasm have relied on QDs being endocytosed by the cell and escaping from the endosome. Osmotic lysis of endosomes,[10,11] endosome escape by positively charged polymers[12–15] and cell-penetrating peptides,[11,16] and liposome-mediated delivery[17] have demonstrated some cytosolic delivery as supported by evidence including diffuse staining patterns on confocal microscopy. Unfortunately, all suffer from some combination of low reproducibility, low cell viability, incomplete endosome escape, and poor delivery efficiency. In addition, such approaches require achieving a well-controlled dual conjugation of an intracellular delivery handle and a cytosolic protein-targeting handle on the same nanoparticle, which can be difficult. Despite reports of reliable cytosolic delivery of gold nanoparticles,[3,18] quantum dots have yet to be delivered into the cell cytoplasm in a robust and scalable manner.[19]

Because QD delivery into the cell cytoplasm has remained difficult, the utility of QD fluorescent labels in cell biology has been limited to fixed cell imaging or membrane protein labeling[1,19] of live cells.[2] Fluorescence microscopy has provided countless insights into cellular architecture, biomolecule interactions, and protein localizations thanks to brighter, more stable fluorophores and fluorescent proteins (FPs). FPs in particular can be genetically encoded, ensuring labeling specificity and proper intracellular localization. However, FPs have shortcomings that may be complemented by the photostability, broad absorption bandwidth, high absorption coefficient, and narrow emission of QDs.[20] For example, QDs are emerging as strong candidates for single-molecule, long-term tracking studies in fluorescence microscopy because QDs provide an order of magnitude higher brightness than FPs and are more photostable.[19,21] Unlike FPs, QDs are exogenous to the cell and thus need a conjugation handle that binds specifically to the protein of interest, in addition to being directed into the cellular compartment where the protein resides. Recent work has addressed the issue of specific conjugation through methods such as antibody targeting, streptavidin-biotin labeling schemes, HaloTag-chloroalkane and acyl carrier protein-acetyl CoA labeling.[6,22] In this report, we address the cytosolic delivery challenge by using a microfluidic device to deliver quantum dots to the cytosol and we confirm their delivery by observing their interaction with the cytosolic environment.

## QD delivery into the cytosol

The microfluidic, intracellular delivery device which we use here to deliver aqueous QDs into the cytosol, and its mechanism of delivery[23] are illustrated in figure 1a–b. In this device, cells are rapidly deformed as they pass through a constriction in a microfluidic channel, thus resulting in the formation of transient membrane disruptions. Macromolecules, such as QDs, may then diffuse into the cytosol during the life-time of these disruptions (Fig 1b).[23] Here we combine this microfluidic device with a new generation of recently described biologically compatible QDs.[24] The QDs used throughout this study were coated with a poly-imidazole ligand (PIL) comprised of multiple metal-chelating imidazole groups and multiple water-solubilizing, passivating poly(ethylene) glycol (PEG).[24] The particular PIL that coated the QDs imaged in figure 1c had no functionality other than providing biocompatibility through PEG groups.[24] Confocal microscopy images show that HeLa cells, detached and round after flowing through the microfluidic device, have diffuse cytoplasmic QD staining throughout different z-sections of the cell (Fig 1c, top). The diffuse staining persists even after 48 hours, following incubation and adherence of the cells at 37 °C in 5% $CO_2$ (Fig. 1c, bottom). The diffuse QD fluorescence is dimmer at 48hrs, likely due to cell division (Fig 1c). The device delivered QDs (~13 nm hydrodynamic diameter) into ~40% of the live cell population at a throughput rate of ~10,000 cells/s (Fig S6C). Cell viability was >80% as measured by flow cytometry (Fig S6A). The viability of treated cells as measured

by flow cytometry, the diffuse staining on the confocal images, and the cell's ability to adhere are consistent with delivery of QDs into the cytoplasm of a live cell.

To confirm that the fluorescence indeed arises from QDs delivered to the cytosol as opposed to QDs sequestered in endosomes, we designed a nanoparticle engineered to change its emission profile upon interaction with the reducing environment of the cytosol. The reduction potential inside the cell cytoplasm is −260 to −220 mV and is primarily dictated by the maintenance of high concentrations (5–10 mM) of the tripeptide glutathione.[25,26] Therefore, by measuring the fluorescence of a QD-dye construct whose emission changes when exposed to the cytosolic environment, we can simultaneously determine the localization and chemical accessibility of the delivered nanoparticles. We engineered a QD-dye construct comprising of a green emitting QD ($\lambda_{emission}$ = 541 nm) that acts as an energy donor to a carboxy-X-Rhodamine (Rox) dye ($\lambda_{emission}$ = 610 nm), conjugated through a reducible disulfide bond (Fig 2a). Thiol groups that were incorporated into the PIL formed disulfide bonds with thiolated Rox dyes. The absorbance spectrum of the purified construct has absorbance features of both QD (green arrow) and Rox (red arrow) (Fig 2b) at an average of 13 Rox dyes per QD, effectively quenching the QD fluorescence (Fig 2c). This construct serves as an irreversible sensor of the specific reducing environment in the cytosol. When the QD is selectively excited by a laser at 488 nm (microscopy) or 405nm (flow cytometry) while the disulfide bridges are intact, the construct undergoes FRET so that Rox emission in the red dominates. In a solution assay, the cellular reductant glutathione cleaves the disulfide bridges, releasing Rox dyes and allowing the QD fluorescence to recover (Fig 2d). The non-thiol based reductant tris-(2carboxyethyl)phosphine also allows QD fluorescence recovery, indicating that the release of Rox from the QD surface is not via PIL displacement by glutathione (Fig 2e). Rox fluorescence may not completely disappear due to some of the disulfide bridges being sterically hindered by long PEG groups on the PIL, and due to some small amount of non-specific interaction between the dye and the QD surface.

Changes in the fluorescence profile of the construct, as measured by flow cytometry and confocal microscopy, were used to confirm the delivery of QD-disulfide-Rox constructs to the cell cytoplasm. When exposed to the reducing cytosolic environment, the cleavage of the disulfide bonds disrupts the FRET process from the QD to the dye. Therefore, upon exclusive excitation of the QD, QD channel fluorescence increases while Rox channel fluorescence decreases with time. Live HeLa cells were treated by the microfluidic device in a solution with a high concentration of QD-disulfide-Rox, incubated for 5 minutes, and washed to remove excess QDs before adding cell culture media (these are referred to below as the treated cells). Control cells were incubated with QD-disulfide-Rox for 5 minutes instead of being treated by the microfluidic device, and washed before being placed in cell culture media (See Supplementary information for procedure and 40 minute incubation control). The Rox and QD channel fluorescence of these treated and control cells were observed by both confocal microscopy and flow cytometry.

Under the confocal microscope, the diffuse fluorescence that appears across the cytoplasm of treated cells progresses from strongly red to strongly green (Fig 3a, top. See supplementary for additional images). Control cell images show some non-specific binding on the outer membrane as demonstrated by the ring-shaped fluorescence, and there is no increase in green channel signals (Fig 3a, bottom). These effects are consistent with the expected cleavage of cytosolic disulfide bonds which reduce the FRET effect. In figure 3b, the line graph plots the average QD and Rox channel intensity per cell after correcting for cell-to-cell differences in delivered fluorescent material by normalizing for total fluorescence, for treated and control cells and autofluorescence. For treated cells, the graph shows a cross over between 2–4 hours of incubation where the QD fluorescence rises above the Rox fluorescence. Interestingly, the treated cell Rox signal is shown to stabilize above

autofluorescence levels after 9 hours. This is consistent with results from solution assays, where some FRET remained after reduction. The observed diffuse staining and increase in QD signal and reduction in Rox signal strongly support cytosolic delivery and subsequent disulfide bond cleavage. The QD fluorescence in control cells, quenched by FRET to the Rox, appears indistinguishable from autofluorescence (Fig 3b, Fig S7). The control cells display some Rox fluorescence above autofluorescence at early time points, which then steadily decreases. This is attributed to non-specific interactions between QD-S-S-Rox and the surface of the cell, followed by re-solvation of the constructs into the medium.

Flow cytometry measurements (Fig 4) confirm that the QD-disulfide-Rox constructs can interact with the cytosolic environment. Flow cytometry measurements were recorded on all live cells, encompassing both delivered (~35% of the treated cell population, Fig S14) and undelivered cells. Figure 4a shows the average fluorescence per cell of the treated and control populations. The average QD fluorescence rises initially for the treated cells, peaking at ~9 hrs and falling gradually thereafter, in contrast to the QD fluorescence of the control cell population, which stays comparable to autofluorescence levels. This is consistent with the cytosolic reduction of disulfide bridges between the QD and dye inside the treated cells followed by dilution of fluorescence constructs by cell division. The Rox fluorescence for both the treated and control cells start high and drop within the first 2 hrs. This drop is attributed to the re-solvation into the medium of particles that had become bound to the cell surface during incubation. The average Rox fluorescence in the treated cell population appears similar to control cells due to the presence of undelivered cells within the treated population. The presence of both delivered and undelivered cells within the treated population can be distinguished in the histograms of QD and Rox intensity (Fig 4b). With increasing time, the fluorescence histograms become bimodal for treated cells but stay unimodal for control cells. QD fluorescence rises with time in a subset of the treated cell population (Fig. 4b, left), further supporting the disruption of the FRET process in the cytosol of treated and delivered cells. Rox fluorescence decreases overall as membrane-bound constructs are re-solvated into the medium, but a subset of the treated cell population retains Rox fluorescence. This is consistent with the incomplete reduction of QD-S-S-Rox bonds observed in confocal microscopy. The viability of the treated cell population, as measured by propidium iodide staining, is within 10% of the control population at all time points (Fig. 4c). Our cell viability of >90% relative to the control group compares favorably to alternative methods such as electroporation and polymer-based methods, which have yielded post-treatment viabilities as variable as 0–50%[27] and low as 40–60%,[28] respectively.

## Single QD tracking in cell cytosol

The QD delivery platform also enabled single molecule imaging by delivering unaggregated QD-disulfide-Rox constructs, as the observed emission intermittency is consistent with single QDs.[29] For this experiment, QD-disulfide-Rox constructs were delivered into the cytosol followed by a 10 hour incubation and imaged on an epifluorescence microscope. The 10 hour incubation ensured that the QD fluorescence from inside the cytosol has recovered via disulfide bond reduction; epifluorescence microscopy was used to ensure that enough photons are collected. We observed several blinking QDs when cells were treated by the device at low QD concentrations (Fig. 5). Intensity traces of blinking QDs in the cytosol, shown in the bottom panel of figure 5, appear non-binary as a result of long acquisition bin times (500 ms). Translational cell movements were deemed minimal during the time frame of the acquisition (~1 min). This proof-of-concept experiment highlights the possibility of observing single molecule events within the cell cytosol by delivering QDs as fluorescent labels using this device.

In summary, we have demonstrated nanoparticle delivery into the cell cytosol using a novel microfluidic device. By observing the cleavage of QD-disulfide-Rox by cytosolic reductants, we show that the nanoparticle surface interacts with cytosolic components. The delivery platform, introduced and explained in full elsewhere,[23] enables us to deliver QDs into the cell cytoplasm at high throughput without any cell penetrating or endosome escaping ligands, or laser ablation,[30] while conserving cell viability and QD integrity. The delivery efficiency of 35% may be further increased by increasing the number of microfluidic constrictions, changing constriction dimensions, or increasing the number of treatment cycles. Unlike most of the current cell penetrating peptide or positive charge-assisted delivery methods, our approach does not require dual conjugation of an intracellular delivery handle and a cytosolic protein-targeting handle on the same nanoparticle. By dispensing the need for the former, we mitigate the concerns of cross-reactivity, unequal reactivity efficiencies of conjugation strategies, and conjugation stoichiometry. Therefore, we garner significant flexibility in QD construct design, paving the way for intracellular protein labeling and tracking. We expect this method to enable cytosolic delivery of many fluorescent nanomaterials with complex designs that target intracellular proteins and organelles through proven protein-targeting strategies such as streptavidin-biotin, HaloTag-chloroalkane, and sortase tagging.[6,22]

## Experimental section

### Preparation of water-soluble QD and QD-disulfide-Rox constructs

CdSe/CdS core–shell quantum dots and Polymeric imidazole ligand (PIL) were synthesized according to previously reports.[24] The PILs used throughout this work were two types: one consisting of 50% methoxy-terminated oligo(ethyleneglycol) sidechains, and 50% histamine sidechains and one consisting of 40% methoxy-terminated oligo(ethyleneglycol) sidechains, 20% lipoic acid sidechains, and 40% histamine sidechains. The native hydrophobic trioctyl phosphine and trioctyl phosphine oxide NC ligands were displaced by PIL following a previously described procedure.[24] Briefly, CdSe/CdS core–shell quantum dots in trioctylphosphine/octadecene were precipitated with acetone and methanol. After centrifugation, the supernatant was discarded and the pellet re-dispersed in chloroform. This solution was added to PIL in chloroform under stirring. After 10 minutes, methanol was added and stirring continued for a further 30 minutes. After this time, the solution was diluted with an ethanol/chloroform mixture (1:1 v/v) and precipitation induced by the addition of hexane. The nanoparticles were collected by centrifugation, and the supernatant discarded. The resulting product was dissolved in water, filtered through a 0.2 μm HT Tuffryn membrane and dialyzed against PBS, pH 7.4 buffer. The concentration of the recovered solution was determined by UV-Vis spectroscopy.

### Cytosolic delivery of QD constructs

The etched silicon wafer was manufactured, cleaned, and processed as described elsewhere; the detailed cytosolic delivery protocol is also described elsewhere.[23] Briefly, for cytosolic delivery, cells were aliquoted into a PBS solution containing QD. The cell-QD solution was pipetted into the microfluidic device and driven through the channels at constant pressure, followed by a 5 min incubation period. After this incubation period, excess QDs were separated by centrifugation. For the control population, the cells were simply exposed to the QD solution for an amount of time equivalent to the cytosolic delivery protocol.

### Confocal microscopy

Images were taken on live cells using the C1 confocal on a Nikon TE2000-U inverted microscope with a 60x water-immersion lens. Fluorescence samples were excited at 488 nm from an argon-Ion laser. Emission was collected with a 585 Long-Pass dichroic mirror for

QD541 fluorescence collection through 535/30 filter and Rox fluorescence collection through a 605/30 filter. A single image is an average from n=8 scans.

### Flow cytometry

Fluorescence was measured using a LSR Fortessa (BD Biosciences). QD constructs were excited at 405 nm and emission was collected with a 525/50 filter for QD541 and a 595 Long-Pass filter for Rox. Dead cells were sorted out from the sample by discarding cells showing propidium iodide fluorescence excited at 488 nm and measured through a 695 Long-Pass filter.

## Supplementary Material

Refer to Web version on PubMed Central for supplementary material.

## Acknowledgments

The work received support from the NIH through grants 5-U54-CA119349-05 (M.G.B.), 5R01CA126642-02 (M.G.B.) and RC1 EB011187-02 (K.F.J.). The Biophysical Instrumentation Facility for the Study of Complex Macromolecular Systems (NSF-0070319, NIH GM68762), the DCIF at MIT (CHE-9808061, DBI-9729592) and the NCI through the Cancer Center Support (core) at MIT (P30-CA14051) are also gratefully acknowledged.

## References

1. Howarth M, Liu W, Puthenveetil S, Zheng Y, Marshall LF, Schmidt MM, Wittrup KD, Bawendi MG, Ting AY. Nature Methods. 2008; 5:397–399. [PubMed: 18425138]
2. Resch-Genger U, Grabolle M, Cavaliere-Jaricot S, Nitschke R, Nann T. Nature Methods. 2008; 5:763–775. [PubMed: 18756197]
3. Verma A, Uzun O, Hu Y, Hu Y, Han H, Watson N, Chen S, Irvine DJ, Stellacci F. Nature Materials. 2008; 7:588.
4. Yum K, Na S, Xiang Y, Wang N, Yu M. Nano Letters. 2009; 9:2193–2198. [PubMed: 19366190]
5. Boukany PE, Morss A, Liao W, Henslee B, Jung H, Yu B, Wang X, Wu Y, Li L, Gao K, Hu X, Hemminger O, Lu W, Lafyatis GP, Lee LJ. Nature Nanotechnology. 2011; 6:747–754.
6. Smith AM, Wen MM, Nie S. Biochem (Lond). 2010; 3:1–12.
7. Biju V, Itoh T, Ishikawa M. Chem Soc Rev. 2010; 39:3031–3056. [PubMed: 20508886]
8. Yoo JS, Kim HB, Bang J, Kim S, Ahn S, Lee BC, Soh KS. Mol Imaging Biol. 2011; 13:471–480. [PubMed: 20567924]
9. Delehanty JB, Bradburne CE, Boeneman K, Susumu K, Farrell D, Mei BC, Blanco-Canosa JB, Dawson G, Dawson PE, Mattoussi H, Medintz IL. Integr Biol 2010. 2010; 2:265–277.
10. Bruchez, MP.; Hotz, CZ. Quantum dots: applications in biology. Humana Press; Totowa: 2007.
11. Courty S, Luccardini C, Yohanns B, Cappello G, Dahan M. Nano Lett. 2006; 6:1491–1495. [PubMed: 16834436]
12. Fuller JE, Zugates GT, Ferreira LS, Ow HS, Nguyen NN, Wiesner UB, Langer RS. Biomaterials. 2008; 29:1526–1532. [PubMed: 18096220]
13. Hu Y, Atukorale PU, Lu JJ, Moon JJ, Um SH, Cho EC, Wang Y, Chen J, Irvine DJ. Biomacromolecules. 2009; 10:756–765. [PubMed: 19239276]
14. Kim BYS, Jiang W, Oreopoulos J, Yip CM, Rutka JT, Chan WCW. Nano Letters. 2008; 8:3887–3892. [PubMed: 18816147]
15. Bayles AR, Chahal HA, Chahal DS, Goldbeck CP, Cohen BE, Helms BA. Nano Letters. 2010; 10:4086–4092. [PubMed: 20831181]
16. Liu BR, Huang Y, Winiarz JG, Chiang H, Lee H. Biomaterials. 2011; 32:3520–3537. [PubMed: 21329975]
17. Dudu V, Ramcharan M, Gilchrist ML, Holland EC, Vazquez M. J Nanosci Nanotechnol. 2008; 8:2293–2300. [PubMed: 18572640]

18. Dhar S, Daniel WL, Giljohann DA, Mirkin CA, Lippard SJ. JACS. 2009; 131:14652–14653.
19. Jaiswal JK, Mattoussi JH, Mauro M, Simon SM. Nature Biotech. 2002; 21:47–51.
20. Medintz IL, Uyeda HT, Goldman ER, Mattoussi H. Nature Materials. 2005; 4:435–446.
21. Patterson G, Davidson M, Manley S, Lippincott-Schwartz J. Rev Phys Chem. 2010; 61:345–67.
22. Zelman-Femiak M, Wang K, Gromova K, Knaus P, Harms GS. Biotechniques. 2010; 49:574–579. [PubMed: 20701592]
23. Sharei A, Zoldan J, Adamo A, Sim WY, Cho N, Jackson E, Mao S, Schneider S, Han M, Lytton-Jean A, Basto PA, Jhunjhunwala S, Lee J, Heller DA, Kang JW, Watson N, Kim K, Anderson DG, Langer R, Jensen KF. Submitted.
24. Liu W, Greytak AB, Lee J, Wong CR, Park J, Marshall LF, Jian W, Curtin PN, Ting AY, Nocera DG, Fukumura D, Jain RK, Bawendi MG. JACS. 2010; 132:472–483.
25. Aw TY. News in Physiological sciences. 2003; 5:201–204. [PubMed: 14500800]
26. Jones DP. Methods Enzymol. 2002; 348:93–112. [PubMed: 11885298]
27. Agarwal A, Zudans I, Weber EA, Olofsson J, Orwar O, Weber SG. Anal Chem. 2007; 79:3589–3596. [PubMed: 17444611]
28. Hong S, Leroueil PR, Janus EK, Peters JL, Kober MM, Islam MT, Orr BG, Baker JR Jr, Banaszak Holl MM. Bioconjugate Chem. 2006; 17:728–734.
29. Pinaud F, Clarke S, Sittner A, Dahan M. Nature Methods. 2010; 7:275–285. [PubMed: 20354518]
30. Chakravarty P, Qian Q, El-Sayed MA, Prausnitz MR. Nat Nanotechnol. 2010; 8:607–611. [PubMed: 20639882]

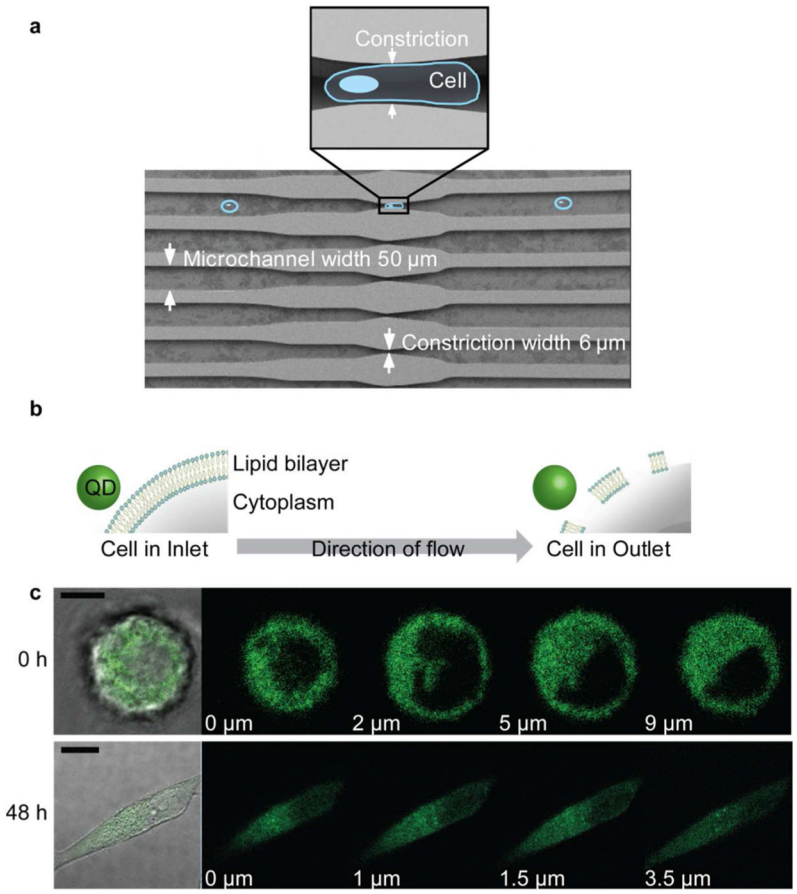


**Figure 1.**

(a) Schematic of the microfluidic device and flow of cells. (b) Hypothesized method of entry for nanoparticles. Images not to scale. (c) Overlay of transmission and confocal fluorescence images, followed by z-section confocal fluorescence images of treated cells delivered with QDs. Top, immediately after treatment and bottom, after 48 h incubation at 37 °C and 5% $CO_2$. The diffuse staining pattern is constrained to the cytoplasm and the nanoparticles appear not to enter the nucleus (dark region within the cell). Scale bar is 10 μm.

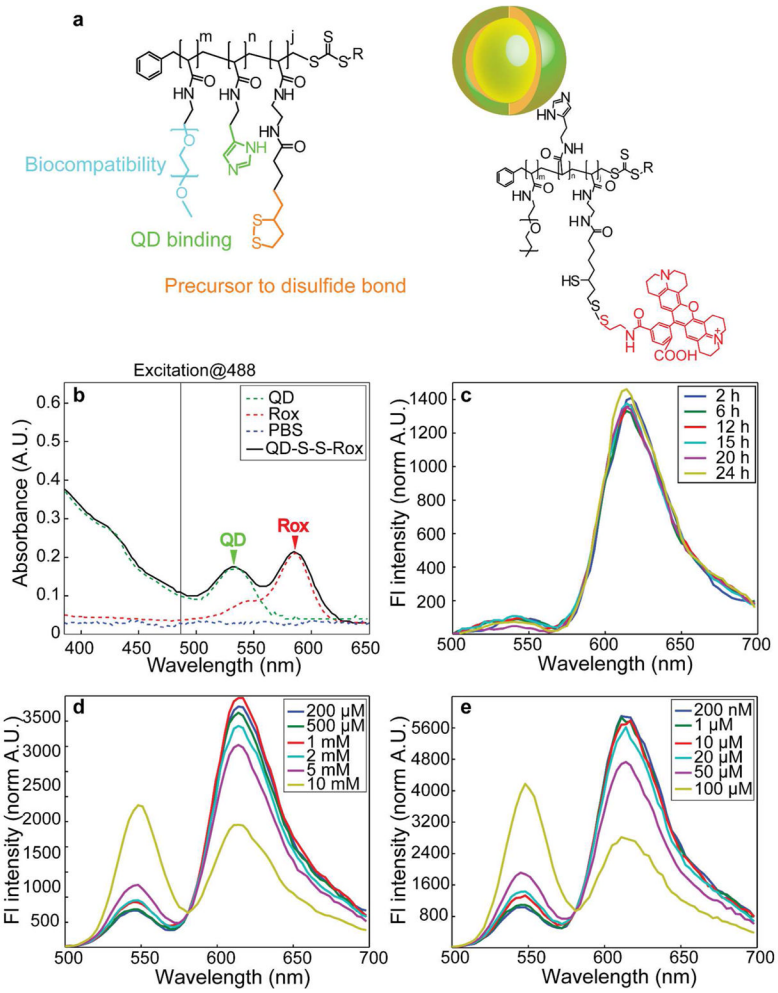


**Figure 2.**

Construct design, absorbance, and stability in various media. (a) A schematic of the free poly-imidazole ligand (PIL) prior to conjugation with the dye and coating the QDs (left), and of the resulting QD-disulfide-Rox construct (right) (image not to scale). (b) The absorbance spectrum of the QD-disulfide-dye construct. Excitation at 488 nm and at 405 nm provided exclusive absorption by the QDs throughout the experiment. (c) The stability of fluorescence energy transfer from QD to Rox for the construct in full culture media at 37 °C and 5% $CO_2$, demonstrating that the disulfide bond is not cleaved in the extracellular environment. (d) Cleavage of the disulfide bond by the cytosolic reductant glutathione, as shown by the recovery of QD fluorescence. (e) Recovery of QD fluorescence upon treatment by the non-thiol reductant tris(2-carboxyethyl)phosphine, further supporting the cleavage of the disulfide bond.

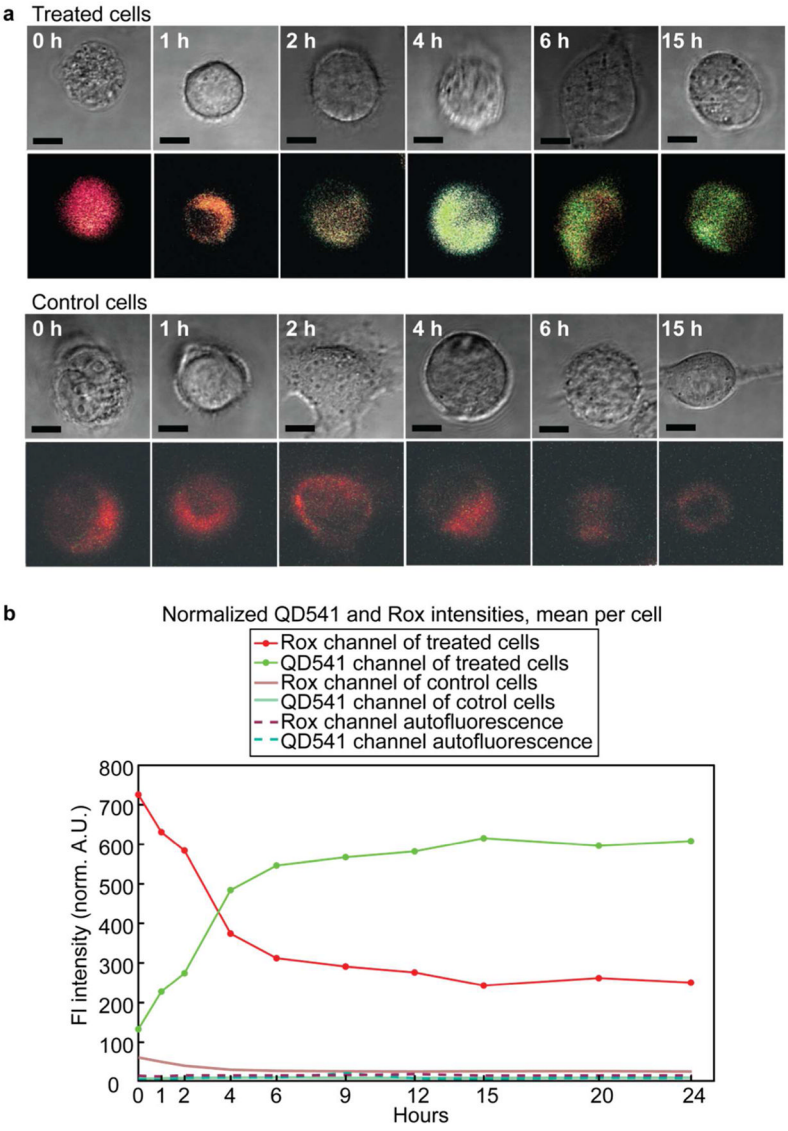


**Figure 3.**

Live cell confocal microscopy images and fluorescence intensity analysis demonstrating cytoplasmic staining and chemical accessibility of QD surface. (a) Images of treated cells (top) and control cells (bottom). The appearance of diffuse green fluorescence is present only in treated cells. Scale bar is 10 μm. (b) Change in intensity as a function of time in the green and red channels. Because n<20 at each time point, fluctuations in total average fluorescence were corrected by normalizing to the 0 h time point. See Supplementary Information for a larger scale line graph of fluorescence in control cells and autofluorescence (Fig S7).

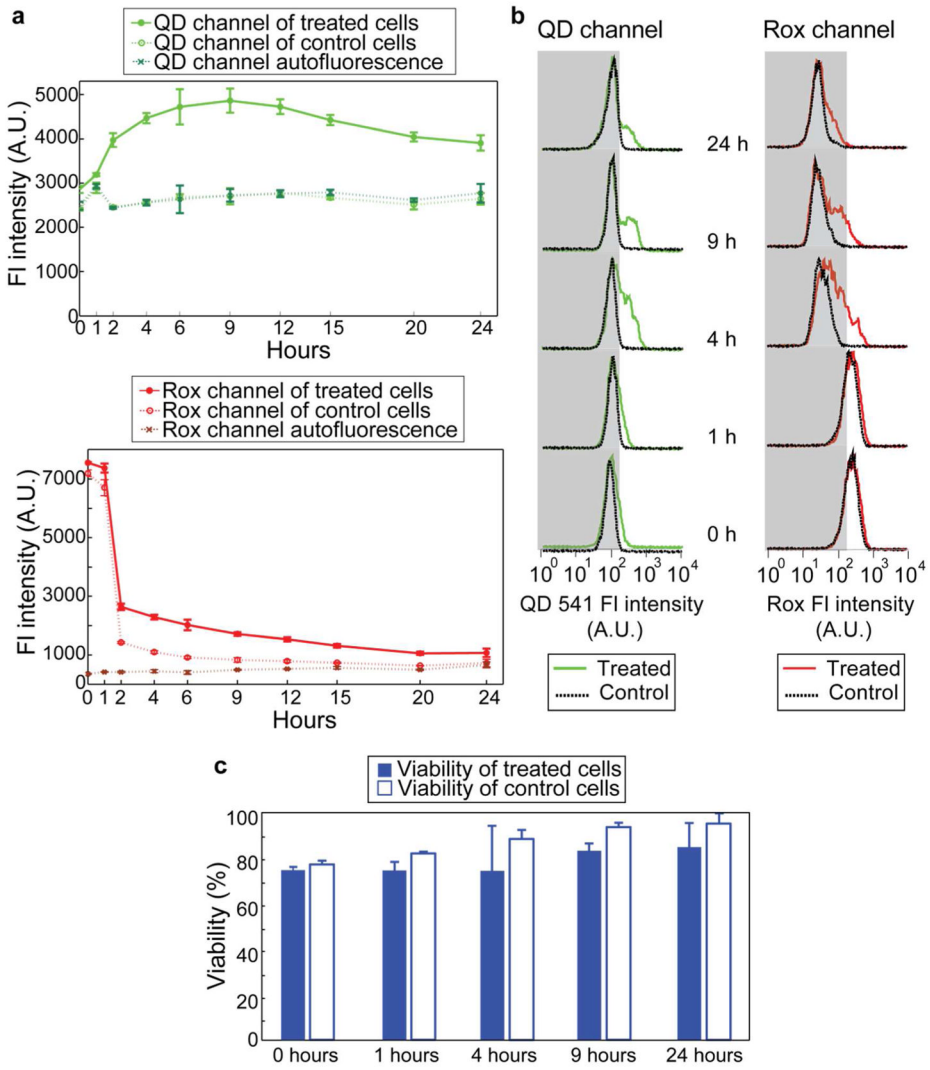


**Figure 4.**

Flow cytometry measurements of average cell fluorescence and viability. (a) Average fluorescence of QD (left) and Rox (right) per cell, showing an increae in QD fluorescence only in treated cells. Rox fluorescence in both treated and control cells is at autofluorescence levels by the 24 h time point. (b) Histogram of the distribution of fluorescence intensities among treated and control cells at select time points, in the QD channel (left) and Rox channel (right). QD delivery is estimated to have occurred in at least 35% of the cell population (Fig S14). Grey areas are meant to guide the eye in the movement of fluorescence intensity histogram peaks. (c) Viability of control and treated cells as measured by propidium iodide.

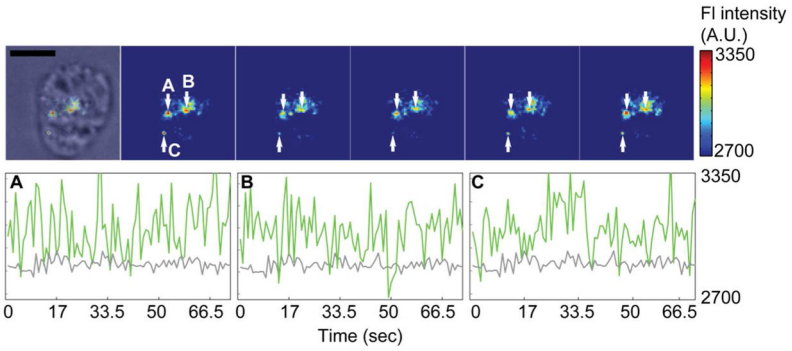


**Figure 5.**

Epifluorescence imaging of unaggregated single QDs within the cell cytosol after device treatment with a 10 nM QD solution (top), and blinking traces of the three QDs labeled A, B, and C (bottom, green lines) with autofluorescence (bottom, grey lines). QD blinking traces appear to be non-binary due to long acquisition bin times (500 ms). Scale bars are 10 μm.